P H Y S I C A L   R E V I E W   L E T T E R S

꿍

Critical Point of an Interacting Two-Dimensional Atomic Bose Gas

Peter Krüger, Zoran Hadzibabic, and Jean Dalibard

Laboratoire Kastler Brossel and CNRS, Ecole Normale Supérieure, 24 rue Lhomond, 75005 Paris, France

We have measured the critical atom number in an array of harmonically trapped two-dimensional (2D) Bose gases of rubidium atoms at different temperatures. We found this number to be about 5 times higher than predicted by the semiclassical theory of Bose-Einstein condensation (BEC) in the ideal gas. This demonstrates that the conventional BEC picture is inapplicable in an interacting 2D atomic gas, in sharp contrast to the three-dimensional case. A simple heuristic model based on the Berezinskii-Kosterlitz-Thouless theory of 2D superfluidity and the local density approximation accounts well for our experimental results.

Bose-Einstein condensation (BEC) at a finite temperature is not possible in a homogeneous two-dimensional (2D) system, but an interacting Bose fluid can nevertheless become superfluid at a finite critical temperature [1]. This unconventional phase transition is described by the Berezinskii-Kosterlitz-Thouless (BKT) theory [2,3], and does not involve any spontaneous symmetry breaking and emergence of a uniform order parameter. It is instead associated with a topological order embodied in the pairing of vortices with opposite circulations; true long-range order is destroyed by long wavelength phase fluctuations even in the superfluid state [4,5].

Recent advances in producing harmonically trapped, weakly interacting (quasi-)2D atomic gases [6–14] have opened the possibility for detailed studies of BKT physics in a controllable environment. There has been some theoretical debate on the nature of the superfluid transition in these systems [15–19] because the harmonic confinement modifies the density of states compared to the homogenous case. This allows for ''conventional'' finite temperature Bose-Einstein condensation in the *ideal* 2D gas [20]. Early experiments have been equally consistent with the BEC and the BKT picture of the phase transition. For example, the density profiles at very low temperatures [6] are expected to be the same in both cases. However, recent studies of matter wave interference of independent 2D atomic clouds close to the transition have revealed both thermally activated vortices [12,13] and quasi–long-range coherence properties [13] in agreement with the BKT theory [21,22].

In this Letter, we study the critical atom number in an array of 2D gases of rubidium atoms, and observe stark disagreement with the predictions of the ideal gas BEC theory. We detect the critical point by measuring (i) the onset of bimodality in the atomic density distribution and (ii) the onset of interference between independent 2D clouds. These two measurements agree with each other, and for the investigated range of temperatures $T \approx 50$–110 nK give critical atom numbers N_c which are ~5 times higher than the ideal gas prediction for conventional Bose-

Einstein condensation in our trap [20]. For comparison, in three-dimensional (3D) atomic gases, where conventional BEC occurs, the increase of the critical atom number due to repulsive interactions is typically on the order of 10% [23,24]. A simple heuristic model based on the BKT theory of 2D superfluidity and the local density approximation gives good agreement with our measurements.

In [13] we studied quasi–long-range coherence of a trapped 2D gas, which is directly related to the *superfluid* density ρ_s. In that case, signatures of the BKT transition emerge only once a significant part of the cloud becomes superfluid. Since the atomic density in the trap is not uniform, this happens slightly below the true critical temperature for the onset of superfluidity in the trap center, and the observed transition is rounded off. The present study concentrates on the exact critical point and relates to the *total* density at criticality ρ_c, which has been of long-standing theoretical interest [25,26].

Our experimental procedure for the preparation of cold 2D Bose gases has been described in [13]. We start with a ^{87}Rb 3D condensate in a cylindrically symmetric magnetic trap with trapping frequencies $\omega_x = 2\pi \times 10.6$ Hz and $\omega_y = \omega_z = 2\pi \times 125$ Hz. To split the sample into 2D clouds we add a blue detuned one-dimensional optical lattice with a period of $d = 3$ μm along the vertical direction z (see Fig. 1). The lattice is formed by two laser beams with a 532 nm wavelength and focused to waists of about 120 μm, which propagate in the yz plane and intersect at a small angle. The depth of the lattice potential around $x = 0$ is $h \times 35$ kHz, corresponding to a vertical confinement of $\omega_z = 2\pi \times 3.0$ kHz. The finite waists of the lattice beams result in a slow variation of ω_z along x, and the variation of the zero point energy $\hbar\omega_z(x)/2$ modifies ω_x to $2\pi \times$ 9.4 Hz at the trap center.

Figure 1 shows contour lines for the full trapping potential. The number of significantly populated lattice planes is ~2–4 in the investigated temperature range (50–110 nK). The vast majority of atoms is trapped in the central x region where the 2D criterion $kT < \hbar\omega_z(x)$ is fulfilled and the tunneling rate between adjacent sites is negligible on the

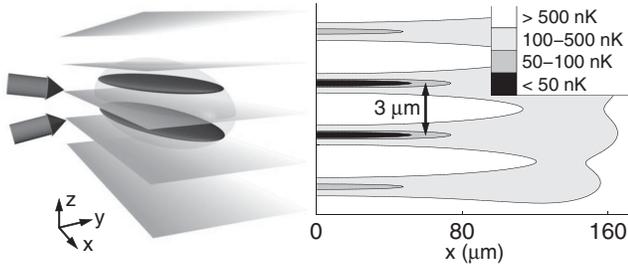P H Y S I C A L   R E V I E W   L E T T E R S

FIG. 1.   Experimental setup. Left: A one-dimensional optical lattice is used to split a magnetically trapped 3D BEC (transparent ellipsoid) into a small array of 2D clouds. Right: Contour lines of the total (magnetic and light) potential $V(x, z)$ in the $y = 0$ plane for the lattice phase such that the two central planes are symmetric with respect to the trap center.

time scale of the experiment. However, the exchange of particles between lattice sites is still possible via the far wings of the energy distribution (at energies above 460 nK). This ensures thermal equilibrium between the planes [27] on the time scale of ~ 100 collision times [28], which in our case corresponds to a fraction of a second. The 2D interaction strength is $g = (\hbar^2/m)\tilde{g}$, where the dimensionless coupling constant $\tilde{g} = a_s\sqrt{8\pi m\omega_z/\hbar} = 0.13$, $a_s = 5.2$ nm is the scattering length, and m the atomic mass [15,29]. The interaction energy $E_{\rm int} \sim g\rho_0$, where ρ_0 is the peak density, also satisfies the 2D criterion $E_{\rm int} < \hbar\omega_z$.

We measure the critical atom number N_c by varying the total atom number N at a fixed temperature. We start with a highly degenerate sample and keep it trapped for a time τ varying between 1 and 10 s. During this time we maintain a constant temperature by applying a constant radio frequency field in the range of 10–25 kHz above the frequency corresponding to the bottom of the trap. As the hold time τ increases, N gradually reduces and drops below N_c due to inelastic losses.

The atomic density profiles are recorded in the xz plane by resonant absorption imaging along y after $t = 22$ ms of time of flight expansion. Along z the profiles are Gaussian, closely corresponding to the zero point kinetic energy $\hbar\omega_z(x = 0)/4$. Along x, for all $N < N_c$ a Gaussian distribution fits the data well [30]. For $N > N_c$, the profiles exhibit a clearly bimodal shape (Fig. 2). The bimodal distributions are fitted well by the sum of a Gaussian, corresponding to the "normal component," and a parabolic Thomas-Fermi (TF) profile expected from superfluid hydrodynamics [23].

From the bimodal fits we extract the total atom number N and the number of atoms within the TF part of the distribution N_0. The absolute detection efficiency of our imaging system was calibrated by measuring critical atom numbers for 3D BECs, taking into account interaction effects [23,24]. For a given energy of the evaporation surface $E_{\rm evap}$ the width of the Gaussian part of the distribution is nearly independent of N (see inset of Fig. 3). For a
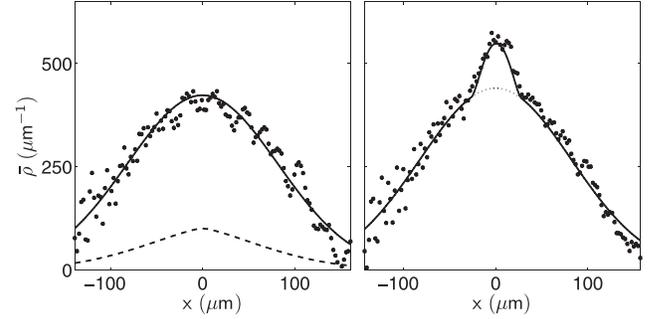

FIG. 2.   Phase transition in a rubidium 2D gas. 2D clouds confined parallel to the xy plane are released from an optical lattice and the density distribution is recorded by absorption imaging along y after $t = 22$ ms of time of flight. The measured line densities $\bar{\rho}(x)$ ($\bullet$) for an atom number just below (left) and just above (right) the critical number are displayed together with bimodal fits (solid lines). The dashed line in the left panel shows the expected distribution of the 2D ideal gas at the threshold of conventional BEC in our potential at the same temperature ($T = 92$ nK). The dotted line in the right panel indicates the Gaussian part of the bimodal distribution.

quasi–non-degenerate gas ($N \sim N_c/2$) this width is given by the temperature. We thus use this estimate for T also in the degenerate regime ($N \gtrsim N_c$), although one could have expected in this regime a deviation from the Gaussian law
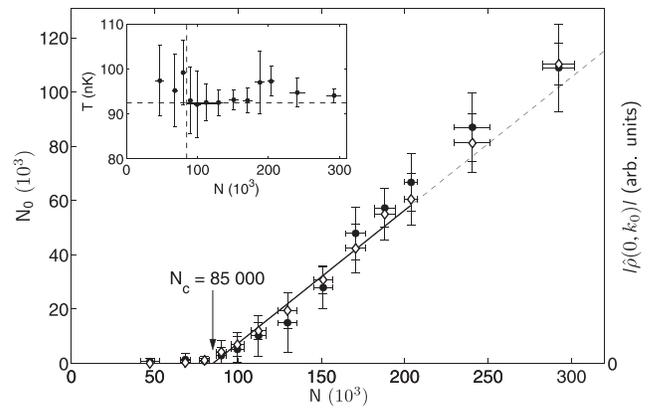

FIG. 3.   Measurement of the critical point. The number of atoms in the Thomas-Fermi part of the bimodal distribution N_0 ($\diamond$) is plotted as a function of the total atom number N. The solid line shows the linear fit we use to determine N_c, and the dashed line is its extrapolation. For comparison, the interference amplitude $|\hat{\rho}(0, k_0)|$ ($\bullet$) is also displayed as a function of N. It shows the same threshold N_c within our experimental precision. The inset shows that the temperature deduced from the Gaussian part of the fit is to a good approximation constant for all data points. Horizontal and vertical dashed lines indicate the average temperature and the critical atom number, respectively. The solid line marks the region used to determine the average temperature $T = 92(6)$ nK close to the transition. Each data point is based on 5–10 images, all error bars represent standard deviations.

for the normal fraction. For example, the ideal gas theory predicts a distribution at the BEC point that is much more peaked at the center of the cloud (Fig. 2). The temperatures inferred in this way scale as $E_{evap} = \eta kT$, with $\eta \approx 10$ compatible with the usual 3D values for evaporation times equal to a few hundred collision times [28]. We estimate the systematic uncertainties of our atom number and temperature calibrations to be 20% and 10%, respectively.

Figure 3 illustrates the threshold behavior of N_0 [31], and Fig. 4 shows the critical numbers N_c measured at four different temperatures. In a single 2D ideal gas, BEC is expected for [20]:

$$N_{c,\mathrm{id}} = \frac{\pi^2}{6}\left(\frac{kT}{\hbar\bar{\omega}}\right)^2, \qquad (1)$$

where $\bar{\omega}$ is the geometric mean of the two trapping frequencies in the plane. For comparison with our experimental results, we have numerically integrated the Bose-Einstein distribution for our confining potential sketched in Fig. 1. The result depends on a 10% level on the exact position of the lattice planes relative to the minimum of the magnetic trap potential. Since we do not fully control this position, we average over the possible configurations. We obtain the result $N_{c,\mathrm{id}}^{\mathrm{multi}} = pN_{c,\mathrm{id}}$, where the effective number of planes p smoothly grows from ≈ 2.2 at 50 nK to ≈ 4.2 at 110 nK. The resulting $N_{c,\mathrm{id}}^{\mathrm{multi}}(T)$ is shown in Fig. 4 as a solid line. Our measurements clearly show systematically higher N_c than expected for ideal gas condensation. An empirical function $N_c = \alpha N_{c,\mathrm{id}}^{\mathrm{multi}}(T)$, with the scaling factor α as the only free parameter, fits the data well and gives $\alpha = 5.3(5)$, where the quoted error is statistical.

We also study the coherent fraction of the 2D gas and compare its behavior with the bimodal density profiles. We investigate the interference patterns that form after releasing the independent planar gases from the trap
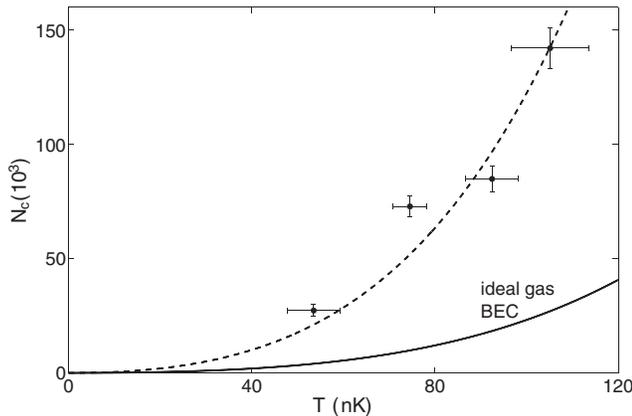
(Fig. 5) [13]. Fourier transforming the density profile $\rho(x, z) \rightarrow \mathcal{F}[\rho(x, z)] \equiv \hat{\rho}(x, k_z)$ allows us to quantify the size of the coherent, i.e., interfering part of the gas as a function of N. The spatial frequency corresponding to the fringe period for the interference of neighboring planes is $k_0 = md/\hbar t$. We find that $|\hat{\rho}(x, k_0)|$ is well fitted by a pure Thomas-Fermi profile. Within our experimental accuracy, the radii $R_{\mathrm{TF}}(k_0)$ of these profiles are equal to those obtained from a bimodal fit to the density. In particular, the onsets of interference and bimodality coincide (circles and diamonds in Fig. 3, respectively).

We now turn to the interpretation of our measurements in the framework of the BKT theory of 2D superfluidity. The theory predicts a universal jump of the *superfluid* density at the transition, from $\rho_s = 0$ to $\rho_s\lambda^2 = 4$, where $\lambda = h/\sqrt{2\pi mkT}$ is the thermal wavelength [21] (for experiments, see [1,13]). However, the *total* density at the critical point ρ_c is not universal because it depends on the microscopic interactions. For weak interactions ($\tilde{g} < 1$), $\rho_c\lambda^2 = \ln(C/\tilde{g})$ [25], with $C = 380 \pm 3$ given by high-precision Monte Carlo calculations [26]. For our value of $\tilde{g} = 0.13$ (experimentally confirmed by measuring R_{TF} as a function of N_0) this gives $\rho_c\lambda^2 = 8.0$.

In a harmonic trap, within the local density approximation, the transition is expected to occur when the density in the center of the cloud reaches the critical value ρ_c. We can heuristically relate the critical density and the corresponding critical atom number $N_{c,\mathrm{BKT}}$ using the experimentally observed Gaussian density profiles. For a single plane with a quadratic confining potential $V(x, y)$, integrating $\rho(x, y) = \rho_c \exp[-V(x, y)/(kT)]$ gives
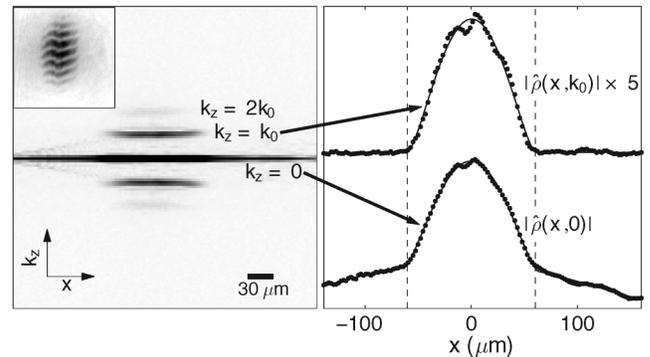
FIG. 5. Coherence and density profile below the transition. Interference of 2D clouds is used to compare the coherent part of the cloud with the part following the Thomas-Fermi density distribution. Left: Interference patterns in the xz plane (see example in inset) are Fourier transformed along the expansion axis z and averaged over ten images taken under identical conditions, to obtain $|\hat{\rho}(x, k_z)|$. Right: Within experimental precision, fits to the total density profile $|\hat{\rho}(x, 0)|$ and the interference amplitude profile $|\hat{\rho}(x, k_0)|$ give the same Thomas-Fermi diameter $2R_{\mathrm{TF}}$, indicated by the dashed lines. The weak second harmonic peak at $k_z = 2k_0$ reveals small occupation of the outer lattice planes.

FIG. 4. Critical point in an interacting 2D gas. The critical atom number N_c (●) is measured at four different temperatures T. Displayed error bars are statistical. The solid line shows the ideal 2D gas BEC prediction $N_{c,\mathrm{id}}^{\mathrm{multi}}$. The dashed line is the best empirical fit to the data, which gives $N_c = \alpha N_{c,\mathrm{id}}^{\mathrm{multi}}$ with $\alpha = 5.3(5)$.

$$N_{c,\text{BKT}} = \rho_c \lambda^2 \left(\frac{kT}{\hbar\bar{\omega}}\right)^2 = \rho_c \lambda^2 \frac{6}{\pi^2} N_{c,\text{id}}. \qquad (2)$$

For $\rho_c \lambda^2 = 8.0$ this gives $N_{c,\text{BKT}}/N_{c,\text{id}} = 4.9$. In a lattice configuration this ratio changes only slightly. We set the peak density in the most populated plane to ρ_c, and sum the contributions of all planes j using the corresponding potentials V_j (here we neglect the small nonharmonic effects due to finite laser waists). The total population in the lattice is then $N_{c,\text{BKT}}^{\text{multi}} = p' N_{c,\text{BKT}}$, where the effective number of planes p' varies from 2.4 at 50 nK to 3.5 at 110 nK. We thus obtain $N_{c,\text{BKT}}^{\text{multi}}/N_{c,\text{id}}^{\text{multi}} \simeq 4.7$, which is close to the experimental ratio $\alpha = 5.3$.

One could try to reproduce our observations within the self-consistent Hartree-Fock (HF) theory [19] (see also [32–34]), by replacing $V(\mathbf{r})$ with the effective mean field potential $V(\mathbf{r}) + 2g\rho(\mathbf{r})$ and again setting the peak density to the BKT threshold ρ_c. For very weak interactions, $\log(1/\tilde{g}) \gg 1$, analytical HF calculation gives critical numbers which are only slightly larger than $N_{c,\text{id}}$ [19]. This approach could in principle be implemented numerically for our value of $\tilde{g}$ and our lattice geometry. However, it has been suggested [35] that treating interactions at the mean field level is insufficient for $\tilde{g} \sim 10^{-1}$, because the interactions are strong enough for the critical region to be a significant fraction of the sample. In future experiments with atomic gases $\tilde{g}$ could be varied between 1 and 10^{-4} using Feshbach resonances, allowing for detailed tests of the microscopic BKT theory and the possible breakdown of the mean field approximation.

In conclusion, we have shown that the ideal gas theory of Bose-Einstein condensation, which is extremely successful in 3D, cannot be used to predict the critical point in interacting 2D atomic gases, where interactions play a profound role even in the normal state. A much better prediction of the critical point is provided by the BKT theory of 2D superfluidity. We have also shown that, despite the absence of true long-range order, the low temperature state displays density profiles and local coherence largely analogous to 3D BECs.

[1] D. J. Bishop and J. D. Reppy, Phys. Rev. Lett. **40**, 1727 (1978).

[2] V. L. Berezinskii, Sov. Phys. JETP **34**, 610 (1972).

[3] J. M. Kosterlitz and D. J. Thouless, J. Phys. C **6**, 1181 (1973).

[4] N. D. Mermin and H. Wagner, Phys. Rev. Lett. **17**, 1133 (1966).

[5] P. C. Hohenberg, Phys. Rev. **158**, 383 (1967).

[6] A. Görlitz et al., Phys. Rev. Lett. **87**, 130402 (2001).

[7] S. Burger, F. S. Cataliotti, C. Fort, P. Maddaloni, F. Minardi, and M. Inguscio, Europhys. Lett. **57**, 1 (2002).

[8] D. Rychtarik, B. Engeser, H.-C. Nägerl, and R. Grimm, Phys. Rev. Lett. **92**, 173003 (2004).

[9] Z. Hadzibabic, S. Stock, B. Battelier, V. Bretin, and J. Dalibard, Phys. Rev. Lett. **93**, 180403 (2004).

[10] N. L. Smith, W. H. Heathcote, G. Hechenblaikner, E. Nugent, and C. J. Foot, J. Phys. B **38**, 223 (2005).

[11] M. Köhl, H. Moritz, T. Stöferle, C. Schori, and T. Esslinger, J. Low Temp. Phys. **138**, 635 (2005).

[12] S. Stock, Z. Hadzibabic, B. Battelier, M. Cheneau, and J. Dalibard, Phys. Rev. Lett. **95**, 190403 (2005).

[13] Z. Hadzibabic, P. Krüger, M. Cheneau, B. Battelier, and J. Dalibard, Nature (London) **441**, 1118 (2006).

[14] I. B. Spielman, W. D. Phillips, and J. V. Porto, Phys. Rev. Lett. **98**, 080404 (2007).

[15] D. S. Petrov, M. Holzmann, and G. V. Shlyapnikov, Phys. Rev. Lett. **84**, 2551 (2000).

[16] D. S. Petrov and G. V. Shlyapnikov, Phys. Rev. A **64**, 012706 (2001).

[17] J. O. Andersen, U. Al Khawaja, and H. T. C. Stoof, Phys. Rev. Lett. **88**, 070407 (2002).

[18] T. P. Simula and P. B. Blakie, Phys. Rev. Lett. **96**, 020404 (2006).

[19] M. Holzmann, G. Baym, J.-P. Blaizot, and F. Laloë, Proc. Natl. Acad. Sci. U.S.A. **104**, 1476 (2007).

[20] V. Bagnato and D. Kleppner, Phys. Rev. A **44**, 7439 (1991).

[21] D. R. Nelson and J. M. Kosterlitz, Phys. Rev. Lett. **39**, 1201 (1977).

[22] A. Polkovnikov, E. Altman, and E. Demler, Proc. Natl. Acad. Sci. U.S.A. **103**, 6125 (2006).

[23] F. S. Dalfovo, L. P. Pitaevkii, S. Stringari, and S. Giorgini, Rev. Mod. Phys. **71**, 463 (1999).

[24] F. Gerbier et al., Phys. Rev. Lett. **92**, 030405 (2004).

[25] D. S. Fisher, and P. C. Hohenberg, Phys. Rev. B **37**, 4936 (1988).

[26] N. Prokof'ev, O. Ruebenacker, and B. Svistunov, Phys. Rev. Lett. **87**, 270402 (2001).

[27] Y. Shin et al., Phys. Rev. Lett. **92**, 150401 (2004).

[28] O. J. Luiten, M. W. Reynolds, and J. T. M. Walraven, Phys. Rev. A **53**, 381 (1996).

[29] Y. Kagan, B. V. Svistunov, and G. V. Shlyapnikov, Sov. Phys. JETP **66**, 314 (1987).

[30] By imaging along x, we verified that the profiles along y are also fitted well by a Gaussian.

[31] Note that the slope $dN_0/dN \sim 0.7$ for $N > N_c$ is less than unity, contrary to what is expected for a saturated gas. This lack of saturation will be discussed elsewhere.

[32] R. K. Bhaduri et al., J. Phys. B **33**, 3895 (2000).

[33] J. P. Fernández and W. J. Mullin, J. Low Temp. Phys. **128**, 233 (2002).

[34] C. Gies and D. A. W. Hutchinson, Phys. Rev. A **70**, 043606 (2004).

[35] N. Prokof'ev and B. Svistunov, Phys. Rev. A **66**, 043608 (2002).